The Chemistry of Sterically Crowded Aryl Oxide Ligands. 3. Crystal and Molecular Structure and Spectroscopic Properties of Mixed Benzyl–Aryl Oxide Compounds of Zirconium[1]

Stanley L. Latesky, Anne K. McMullen, Gerald P. Niccolai, and Ian P. Rothwell*

Department of Chemistry, Purdue University, West Lafayette, Indiana 47907

John C. Huffman

Molecular Structure Center, Indiana University, Bloomington, Indiana 47405

Received November 21, 1984

The reaction between tetrabenzyl- or tetrakis(4-fluorobenzyl)zirconium, $Zr(CH_2Ph)_4$ or $Zr(CH_2PhF)_4$, and the sterically demanding ligand 2,6-di-*tert*-butylphenol (HOAr′) leads to two types of substitution products: $Zr(OAr')(CH_2Ph)_3$ (Ia), $Zr(OAr')(CH_2PhF)_3$ (Ib), and $Zr(OAr')_2(CH_2Ph)_2$ (IIa), $Zr(OAr')_2(CH_2PhF)_2$ (IIb). Addition of 4-methoxy-2,6-di-*tert*-butylphenol (HOAr′–OMe) to Ia generates the mixed aryl oxide $Zr(OAr')(OAr'–OMe)(CH_2Ph)_2$ (IIc). Structural studies show that I contains a significant interaction between the zirconium atom and the aryl ring of one of the benzyl groups which is best described as approaching η^3-bonding, whereas the ligands in II are purely σ-bound (η^1). Spectroscopic evidence (^1H and ^{13}C NMR) suggests the possible retention of this type of interaction in solution. Compound Ia crystallizes in space group $C2/c$ with a = 17.499 (10) Å, b = 10.566 (6) Å, c = 32.769 (12) Å, β = 95.79 (2)°, and Z = 8. Compound Ib crystallizes in space group $P2_1/c$ with a = 9.480 (3) Å, b = 33.605 (19) Å, c = 10.608 (4) Å, β = 114.20 (2)°, and Z = 4. Compound IIc crystallizes in space group $P2_1/n$ with a = 17.683 (9) Å, b = 11.342 (5) Å, c = 19.470 (1) Å, β = 101.01 (2)°, and Z = 4.

Introduction

The chemistry of the benzyl ligand in transition-metal organometallic chemistry is separated from that of simple alkyl groups by its potential to undergo bonding to the metal through the π-orbitals of the aromatic ring.[2] The resulting mode of coordination is now well established for middle and later transition metals, and many studies of the fluxional behavior of such groups have been carried out.[3] Typically this η^3-mode is favored when the benzyl group is attached to a metal center that would be two-electron deficient in the absence of any π-donation from the aryl group. An η^5-bonding mode has recently been proposed for a rhodium system.[4]

However, another type of multisite bonding of the benzyl ligand has been observed on high-valent early-transition metal centers. Initial recognition of this type of interaction came from the solid-state structures of the homoleptic $M(CH_2Ph)_4$ (M = Ti, Zr, Hf) compounds.[5] A similar situation has recently been shown to occur in the organoactinides $Cp^*Th(CH_2Ph)_3$ ($Cp^* = \eta^5$-C_5Me_5),[6] $Th(CH_2Ph)_4(Me_2PCH_2CH_2PMe_2)$, and $U(CH_2Ph)_3Me(Me_2PCH_2CH_2PMe_2)$.[7] During our studies of early-transition-metal aryl oxide chemistry[8] we have isolated a series of mixed benzyl–aryloxy species of zirconium. Analysis of these compounds has allowed us to investigate more fully the structural and spectroscopic characteristics of this latter type of interaction to zirconium. Furthermore, structural studies have allowed us to more clearly characterize the bonding properties of the sterically very demanding ligand 2,6-di-*tert*-butyl phenoxide in these systems. This is of significance given the mild intramolecular activation of the aliphatic CH bonds of the ligand (cyclometalation) that has been demonstrated in some of these compounds.[1,8]

Results

Addition of the sterically demanding ligand 2,6-di-*tert*-butylphenol (HOAr′, 1 equiv) to either $Zr(CH_2Ph)_4$ or $Zr(CH_2PhF)_4$ (CH_2PhF = 4-fluorobenzyl) in toluene solvent leads to the clean formation of the monosubstituted compounds $Zr(OAr')(CH_2Ph)_3$ (Ia) and $Zr(OAr')(CH_2PhF)_3$ (Ib). Further reaction with HOAr′ is slow, but on exposure to excess phenol for days at 25 °C I converts to the disubstituted $Zr(OAr')_2(CH_2Ph)_2$ (**IIa**) and $Zr(OAr')_2(CH_2PhF)_2$ (IIb). Similarly, reaction of tris(benzyl) Ia with 4-methoxy-2,6-di-*tert*-butylphenol (4-OAr′–OMe) results in the high yield formation of the mixed aryl oxide $Zr(OAr')(OAr'–OMe)(CH_2Ph)_2$ (IIc). Both I and II are pale yellow solids, and both are less susceptible to light than the parent tetraalkyl. Wolczanski has shown that reaction of the sterically demanding alcohol tri-*tert*-butylmethanol (tritox) with $Zr(CH_2Ph)_4$ leads to the complex $Zr(tritox)(CH_2Ph)_3$ and 1 equiv of toluene.[9]

In order to more fully characterize these complexes and to try and correlate their spectroscopic properties (vide

(1) For part 2, see: Chamberlain, L.; Keddington, J.; Huffman, J. C.; Rothwell, I. P. *Organometallics* **1982**, *1*, 1513.
(2) (a) Cotton, F. A.; La Prade, M. D. *J. Am. Chem. Soc.* **1968**, *90*, 5418. (b) Bleeke, J. R.; Burch, R. R.; Coulman, C. L.; Schardt, B. C. *Inorg. Chem.* **1981**, *20*, 1316. (c) Sonada, A.; Bailey, P. M.; Maitlis, P. M. *J. Chem. Soc., Dalton Trans.* **1979**, 346.
(3) (a) Cotton, F. A.; Marks, T. J. *J. Am. Chem. Soc.* **1969**, *91*, 1339. (b) Roberts, J. S.; Klabunde, K. J. *J. Am. Chem. Soc.* **1977**, *99*, 2509. (c) Becker, Y.; Stille, J. K. *J. Am. Chem. Soc.* **1978**, *100*, 845.
(4) Burch, R. R.; Muetterties, E. L.; Day, V. W. *Organometallics* **1982**, *1*, 188.
(5) (a) Davis, G. R.; Jarvis, J. A. J; Kilbourn, B. T.; Piols, A. J. P. *J. Chem. Soc., Chem. Commun.* **1971**, 677. (b) Davis, G. R.; Jarvis, J. A. J.; Kilbourn, B. T. *J. Chem. Soc., Chem. Commun.* **1971**, 1511.
(6) Mintz, E. A.; Moloy, K. G.; Marks, T. J.; Day, V. W. *J. Am. Chem. Soc.* **1982**, *104*, 4692.
(7) Edwards, P. G.; Andersen, R. A.; Zalkin, A. *Organometallics* **1984**, *3*, 293.
(8) (a) Chamberlain, L.; Keddington, J.; Huffman, J. C.; Rothwell, I. P. *J. Chem. Soc., Chem. Commun.* **1982**, 805. (b) Chamberlain, L.; Rothwell, I. P.; Huffman, J. C. *J. Am. Chem. Soc.* **1982**, *104*, 7338. (c) Chamberlain, L.; Keddington, J.; Huffman, J. C.; Rothwell, I. P. *Organometallics* **1982**, *1*, 1538. (d) McMullen, A. K.; Rothwell, I. P., results to be published.
(9) Lubben, T. V.; Wolczanski, P. T.; Van Duyne, G. D. *Organometallics* **1984**, *3*, 977.

0276-7333/85/2304-0902$01.50/0

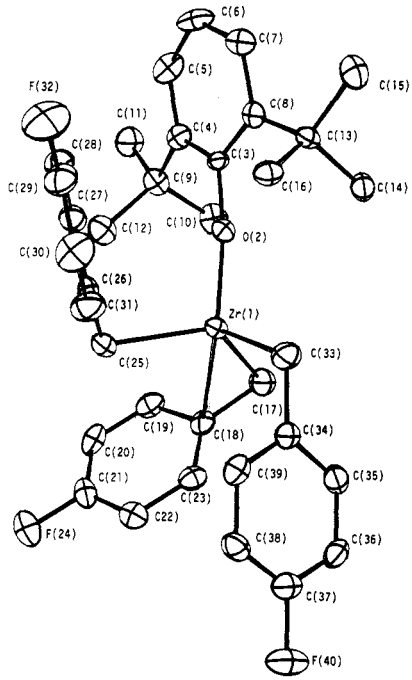

Figure 1. ORTEP view of $Zr(OAr')(CH_2PhF)_3$ (Ib) with hydrogen atoms omitted.

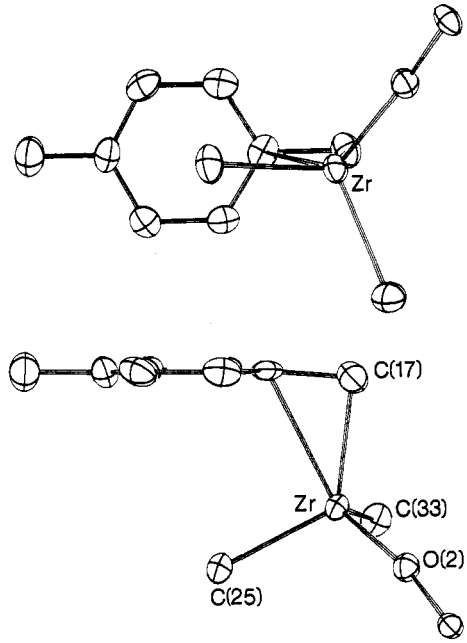

Figure 2. ORTEP views emphasizing the central coordination geometry about the Zr atom in $Zr(OAr')(CH_2PhF)_3$ (Ib). A view both perpendicular to the multibonded benzyl and parallel to the plane of this group is given.

infra) with their structures, single-crystal X-ray diffraction studies were attempted on Ia, Ib, and IIc. Considerable problems were encountered with the refinement of the structure of Ia despite a number of data sets being collected. (See Experimental Section.) However, use of the fluoro analogue Ib yielded a much better result.

Structure of $Zr(OAr')(CH_2PhF)_3$ (Ib). Figure 1 shows an ORTEP view of Ib along with the numbering scheme used. Crystal data are presented in Table I while final coordinates are presented in Table II. Some important bond lengths and angles are given in Table III. It can be seen that the metal maintains a mononuclear environment surrounded by the aryl oxide ligand and three benzyl groups. The Zr–O bond length to the aryl oxide is short, 1.934 (3) Å, implying the presence of some oxygen p to zirconium d π-bonding. The very large Zr–O–Ar' angle of 169.4 (3)° is consistent with this although such angles are characteristic of the coordination properties of this bulky ligand.[8] Of more interest to this study are the coordination characteristics of the benzyl groups. In the solid state the three can be seen to be nonequivalent. There is some unique character to one of the benzyl ligands. This group, bound through C(17), can be seen to have an acute Zr–C–Ph angle of 88° in contrast to 105.4° and 111.6° for the other two. This results in the close proximity of the phenyl ring, and in particular the ipso carbon, to the metal with Zr–C(18) being 2.64 Å. The coordination of the benzyl ligand to the zirconium atom is emphasized in Figure 2.

Clearly there appears to be a significant bonding situation to the aromatic carbons as well as the α-carbon. The geometry about the metal is best described as tetrahedral, as defined by the oxygen and three α-carbons, but with some distortions due to steric effects and also the multisite bonding of the unique benzyl (Table III).

Structure of $Zr(OAr')(CH_2Ph)_3$ (Ia). As mentioned previously we have encountered considerable problems in the determination of the solid state structure of this compound. A number of data sets have been collected but with consistently poor results. However, because of the success achieved with the related complex Ib, we have included the best results we have obtained for Ia. Although of less than ideal quality, we fell that the consistency with that

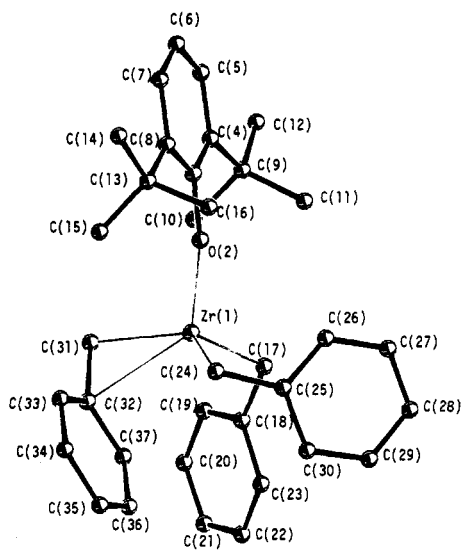

Figure 3. ORTEP view of $Zr(OAr')(CH_2Ph)_3$ (Ia). Due to the poor nature of the thermal elipsoides, atoms are represented by spheres.

of Ib justifies the inclusion of this structure. Figure 3 shows a view of Ia with the numbering scheme used. Crystal data is presented in Table I, while Table IV contains some important bond lengths and angles.

Similarity between the structures of Ia with that of Ib is evident. A unique benzyl group is present with an acute Zr–C–Ph angle of 84° compared to 98° and 115° for the other two benzyls. Again the unique benzyl represents a multisite bonding situation in an approximately tetrahedral metal environment.

Structure of $Zr(OAr')(OAr'\text{–}OMe)(CH_2Ph)_2$ (IIc). Figure 4 shows an ORTEP view of IIc with the numbering scheme used. Tables V and VI contain the structural parameters of the molecule. The geometry about the metal is tetrahedral with a slight distortion due to the steric influence of the aryl oxide ligands causing a squeezing together of the two benzyl α-carbons C(22)–Zr–C(9) = 101.0°. The Zr–O distances, 1.903 (4) and 1.936 (4) Å, and large Zr–O–Ar' angles, 175.4 (4) and 175.7 (4)°, are similar

Table I. Summary of the Crystallographic Data for the Compounds Ia–c

	Ia	IIc	Ib
formula	$ZrC_{35}H_{42}O$	$ZrC_{44}H_{58}O_2$	$ZrC_{35}H_{39}OF_3$
fw	569.94	684.12	623.91
space group	$C2/c$	$P2_1/n$	$P2_1/c$
a, Å	17.499 (10)	17.683 (9)	9.480 (3)
b, Å	10.566 (6)	11.342 (5)	33.605 (19)
c, Å	32.769 (12)	19.470 (11)	10.608 (2)
β, deg	95.79 (2)	101.01 (2)	114.20 (2)
Z	8	4	4
V, Å^3	6027.61	3832.78	3082.52
d(calcd), g/cm^3	1.256	1.238	1.344
cryst size, mm	0.22 × 0.23 × 0.26	0.12 × 0.13 × 0.22	0.12 × 0.14 × 0.14
cryst color	pale yellow	colorless	dark yellow
radiatn		Mo Kα (λ = 0.710 69 Å)	
linear abs coeff, cm^{-1}	3.808	3.157	3.915
temp, °C	−160	−160	−158
detector aperture		3.0 mm wide × 4.0 mm high	
		22.5 cm from crystal	
sample to source dist, cm		23.5	
takeoff angle, deg		2.0	
scan speed, deg/min		4.0	
scan width, deg		2.0 + 0.692 tan θ	
bkgd counts, s		3 at each end of scan	
2θ range, deg		6-45	
data collected	4288	5701	4313
unique data	3943	5031	4046
unique data with $F_p > 2.33\sigma(F)$	1;735	3.708[a]	3.175
$R(F)$	0.0682	0.0658	0.0410
$R_w(F)$	0.0628	0.0661	0.0420
goodness of fit	1.160	1.404	0.929
largest Δ/σ	0.05	0.05	0.05

[a] Unique data with $F_o > 3.00\sigma(F)$.

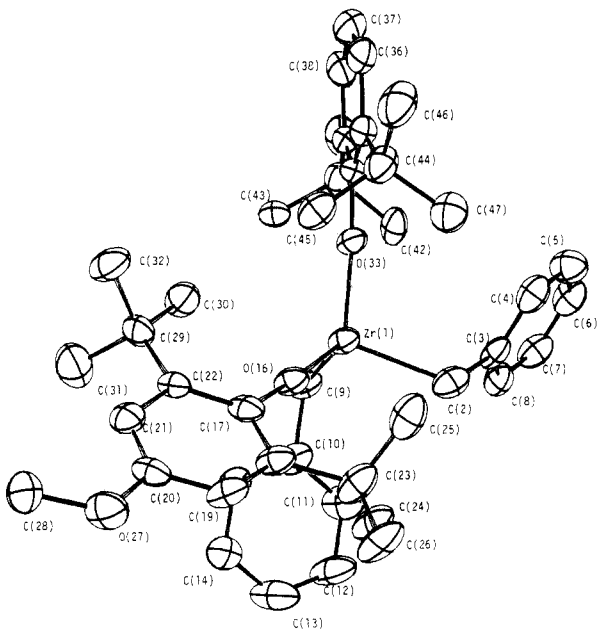

Figure 4. ORTEP view and numbering scheme for Zr(OAr′)(OAr′–OMe)$(CH_2Ph)_2$.

to that seen in I. However, the benzyl ligands can now be considered purely σ-bound to the metal with Zr–C–Ph angles of 107° and 117°.

Spectroscopic Data for I and II. Table VIII contains the collected ^1H and ^{13}C NMR data for $Zr(CH_2Ph)_4$, $Zr(CH_2PhF)_4$, and the new compounds Ia, Ib, IIa, IIb, and IIc.

Discussion

Coordination Properties of 2,6-Di-*tert*-butyl Phenoxide. The bonding characteristics of this ligand are of interest especially in view of the fact that mild thermolysis of compounds II leads to the elimination of 1 equiv of toluene (or 4-fluorotoluene) and cyclometalation of the OAr′ ligand.[8d] The reaction involves the activation of a CH bond of one of the *tert*-butyl groups leading to the formation of a six-membered chelate ring. It can be seen (Figures 1–4) that the large steric pressure caused by the *tert*-butyl groups of the OAr′ ligand is relieved slightly by the formation of almost linear Zr–O–Ar′ angles. The ligand can be seen to occupy a wedge of the coordination sphere, this wedge being defined by the plane of the aromatic ring.

Complex IIc allows one to directly compare the coordination properties of the two ligand OAr′ and OAr′–OMe to see if the presence of a *p*-methoxy substituent in the latter has any significant effect. One might imagine that this strongly electron-donating group would have the effect of enhancing any oxygen to metal d π-bonding, resulting in a shorter metal–oxygen distance. However, although this bond is 0.033 Å shorter than that to the unsubstituted OAr′, the difference is not dramatic.

However, there is an interesting difference to one aspect of the coordination geometry of the OAr′–4-OMe compared to OAr′. This relates to another important factor that determines the steric pressure that these ligands exert at the metal center—the conformation of the *tert*-butyl groups. The minimum steric interaction would occur when the methyl groups are arranged so that a unique methyl group is pointing directly away from the metal center. In this conformation the two remaining methyl groups are equidistant from the metal. This is the geometric configuration adopted by OAr′ in Ia and Ib (Figures 1 and 3) and also by this ligand in IIc (Figure 4). However, for OAr′–OMe although one of the *tert*-butyl groups adopts this conformation, the other adopts the direct opposite. This point is highlighted in Figure 5. In this rotamer one of the methyl groups, C(30), is pointing directly toward the metal, a situation that would be expected to maximize unfavorable steric interactions. This results in a distance to this carbon atom, Zr–C(30), of 3.26 Å compared to 3.92 and 3.96 Å for the closest contacts to the methyl carbons

Table II. Fractional Coordinates and Isotropic Thermal Parameters for $Zr(OAr')(CH_2Ph\text{-}F)_3$ (Ib)

atom	10^4x	10^4y	10^4z	$10B_{iso}$, Å^2
Zr(1)	1945 (1)	8525.6 (1)	2451.8 (5)	16
O(2)	1876 (3)	8753 (1)	4100 (3)	17
C(3)	1917 (5)	8978 (1)	5197 (4)	16
C(4)	3243 (5)	8957 (1)	6474 (5)	20
C(5)	3331 (6)	9233 (2)	7479 (5)	25
C(6)	2152 (7)	9499 (2)	7281 (5)	28
C(7)	806 (6)	9481 (2)	6104 (5)	24
C(8)	630 (5)	9220 (1)	5021 (5)	17
C(9)	4498 (5)	8635 (1)	6806 (5)	21
C(10)	5477 (6)	8682 (2)	5971 (6)	27
C(11)	5627 (6)	8648 (2)	8350 (6)	28
C(12)	3740 (6)	8222 (2)	6566 (6)	25
C(13)	−900 (5)	9213 (1)	3738 (5)	19
C(14)	−685 (6)	9411 (2)	2531 (5)	21
C(15)	−2197 (6)	9446 (2)	3941 (6)	26
C(16)	−1516 (6)	8785 (2)	3406 (6)	21
C(17)	2081 (7)	7859 (2)	2739 (6)	25
C(18)	3401 (6)	7862 (1)	2358 (5)	21
C(19)	3189 (6)	7887 (1)	972 (5)	21
C(20)	4423 (6)	7918 (1)	599 (5)	23
C(21)	5877 (6)	7942 (2)	1624 (5)	24
C(22)	6173 (6)	7920 (2)	3006 (6)	25
C(23)	4941 (6)	7887 (2)	3365 (6)	25
F(24)	7110 (3)	7975 (1)	1270 (3)	33
C(25)	3762 (6)	8884 (2)	2070 (6)	22
C(26)	3325 (5)	9309 (1)	2100 (5)	19
C(27)	3668 (6)	9518 (2)	3334 (5)	21
C(28)	3205 (6)	9907 (2)	3365 (6)	25
C(29)	2394 (6)	10091 (2)	2137 (6)	29
C(30)	2026 (7)	9910 (2)	890 (6)	33
C(31)	2507 (7)	9521 (2)	886 (6)	28
F(32)	1927 (4)	10479 (1)	2149 (4)	44
C(33)	−312 (6)	8628 (2)	608 (5)	24
C(34)	−337 (5)	8426 (1)	−647 (5)	19
C(35)	−873 (5)	8037 (2)	−994 (5)	22
C(36)	−888 (6)	7849 (2)	−2157 (5)	23
C(37)	−352 (5)	8056 (2)	− 2980 (5)	23
C(38)	186 (6)	8434 (2)	−2701 (5)	22
C(39)	188 (6)	8620 (2)	−1526 (5)	21
F(40)	−378 (4)	7875 (1)	−4154 (3)	34

Table III. Selected Bond Distances (Å) and Angles (deg) for $Zr(OAr')(CH_2PhF)_3$ (Ib)

Bond Distances

Zr(1)-O(2)	1.934 (3)	Zr(1)-C(25)	2.270 (5)
Zr(1)-C(17)	2.257 (5)	Zr(1)-C(33)	2.256 (5)
Zr(1)-C(18)	2.640 (5)		

Bond Angles

O(2)-Zr-C(17)	107.0 (2)	C(17)-Zr-C(25)	123.0 (2)
O(2)-Zr-C(25)	105.1 (2)	C(17)-Zr-C(33)	104.5 (2)
O(2)-Zr-C(33)	110.6 (2)	C(25)-Zr-C(33)	106.5 (2)
Zr-O(2)-C(3)	169.4 (3)	Zr-C(25)-C(26)	105.4 (3)
Zr-C(17)-C(18)	88.0 (3)	Zr-C(33)-C(34)	111.6 (3)

Table IV. Selected Bond Distances (Å) and Angles (deg) for $Zr(OAr')(CH_2Ph)_3$ (Ia)

Bond Distances

Zr(1)-O(2)	1.942 (9)	Zr(1)-C(31)	2.276 (15)
Zr(1)-C(17)	2.296 (16)	Zr(1)-C(32)	2.591 (17)
Zr(1)-C(24)	2.26 (17)		

Bond Angles

O(2)-Zr-C(17)	107.4 (6)	C(24)-Zr-C(31)	120.9 (6)
O(2)-Zr-C(24)	102.9 (5)	C(24)-Zr-C(32)	89.7 (6)
O(2)-Zr-C(31)	102.7 (5)	C(31)-Zr-C(32)	34.7 (5)
O(2)-Zr-C(32)	128.5 (5)	Zr-O(2)-C(3)	165.7 (9)
C(17)-Zr-C(24)	111.7 (7)	Zr-C(17)-C(18)	115.1 (11)
C(17)-Zr-C(31)	109.7 (6)	Zr-C(24)-C(25)	97.9 (12)
C(17)-Zr-C(32)	113.7 (6)	Zr-C(31)-C(32)	84.3 (9)

on the opposite *tert*-butyl group. The reason for the adoption of this particular conformation is unclear.

Table V. Fractional Coordinates and Isotropic Thermal Parameters for $Zr(OAr')(OAr'\text{-}OMe)(CH_2Ph)_2$ (IIc)

atom	10^4x	10^4y	10^4z	$10B_{iso}$, Å^2
Zr(1)	98.5 (4)	64 (1)	2712.5 (4)	27
C(2)	506 (4)	−1402 (7)	2101 (5)	36
C(3)	−82 (4)	−2173 (6)	1692 (4)	31
C(4)	−453 (5)	−1901 (7)	1012 (5)	37
C(5)	−1036 (5)	−2582 (8)	648 (5)	43
C(6)	−1256 (5)	−3588 (7)	942 (5)	40
C(7)	−919 (5)	−3896 (8)	1601 (5)	40
C(8)	−340 (5)	−3202 (7)	1975 (4)	35
C(9)	−295 (5)	−964 (7)	3582 (4)	33
C(10)	428 (4)	−1397 (7)	4071 (4)	35
C(11)	759 (5)	−2450 (8)	3967 (6)	49
C(12)	1416 (5)	−2848 (8)	4423 (6)	54
C(13)	1757 (5)	−2175 (9)	4959 (6)	56
C(14)	1474 (6)	−1078 (9)	5061 (5)	56
C(15)	814 (6)	−681 (9)	4607 (5)	51
O(16)	947 (2)	1017 (4)	3134 (3)	29
C(17)	1528 (4)	1790 (6)	3448 (4)	30
C(18)	2283 (4)	1581 (6)	3350 (4)	31
C(19)	2857 (4)	2319 (7)	3686 (4)	34
C(20)	2697 (4)	3240 (6)	4101 (4)	29
C(21)	1968 (4)	3457 (7)	4162 (4)	31
C(22)	1332 (4)	2730 (6)	3847 (4)	25
C(23)	2484 (4)	591 (7)	2885 (5)	39
C(24)	3345 (5)	578 (8)	2834 (6)	48
C(25)	2059 (5)	740 (8)	2134 (5)	42
C(26)	2341 (5)	−634 (7)	3191 (5)	42
O(27)	3333 (3)	3893 (5)	4395 (3)	41
C(28)	3194 (5)	4824 (8)	4851 (5)	45
C(29)	550 (4)	3098 (7)	3981 (4)	32
C(30)	−155 (5)	2321 (8)	3680 (5)	39
C(31)	569 (6)	3174 (10)	4777 (5)	54
C(32)	356 (5)	4349 (7)	3678 (5)	45
O(33)	−718 (2)	858 (4)	2076 (2)	27
C(34)	−1291 (4)	1495 (6)	1656 (4)	27
C(35)	−1084 (5)	2356 (6)	1207 (4)	34
C(36)	−1689 (6)	3012 (8)	802 (5)	44
C(37)	−2435 (5)	2824 (9)	849 (5)	49
C(38)	−2624 (5)	1951 (9)	1290 (4)	43
C(39)	−2055 (4)	1246 (7)	1682 (4)	33
C(40)	−2297 (4)	267 (7)	2133 (4)	37
C(41)	−3182 (4)	35 (10)	1985 (5)	49
C(42)	−1967 (5)	−937 (8)	1989 (5)	38
C(43)	−2077 (4)	581 (8)	2904 (4)	33
C(44)	−247 (5)	2563 (7)	1104 (4)	37
C(45)	253 (5)	3021 (7)	1781 (5)	36
C(46)	−187 (6)	3505 (8)	536 (5)	50
C(47)	104 (5)	1433 (8)	872 (5)	40

Table VI. Selected Bond Distances (Å) and Angles (deg) for $Zr(OAr')(OAr'\text{-}OMe)(CH_2Ph)_2$ (IIc)

Bond Distances

Zr(1)-O(16)	1.903 (4)	Zr(1)-C(2)	2.243 (9)
Zr(1)-O(33)	1.936 (4)	Zr(1)-C(9)	2.272 (8)

Bond Angles

O(16)-Zr-O(33)	116.2 (2)	C(2)-Zr-C(9)	110.0 (3)
O(16)-Zr-C(2)	110.1 (3)	Zr-O(16)-C(17)	175.4 (4)
O(16)-Zr-C(9)	107.4 (3)	Zr-O(33)-C(34)	175.7 (4)
O(33)-Zr-C(2)	106.3 (3)	Zr-C(9)-C(10)	107.0 (5)
O(33)-Zr-C(9)	114.8 (2)	Zr-C(2)-C(3)	117.6 (5)

Space-filling diagrams indicate no reason why rotation of this *tert*-butyl group could not readily take place to give the other conformation. There is now a large body of literature dealing with ground-state M-H-C type interactions.[10] Furthermore, Andersen has characterized a ground-state interaction between a methyl group and ytterbium in the complex $Yb[N(SiMe_3)_2]_2(dmpe)$.[11] It is

(10) Brookhart, M.; Green, M. L. H. *J. Organomet. Chem.* **1983**, *250*, 395 and references therein.
(11) Tilley, T. D.; Andersen, R. A.; Zalkin, A. *J. Am. Chem. Soc.* **1982**, *104*, 2154.

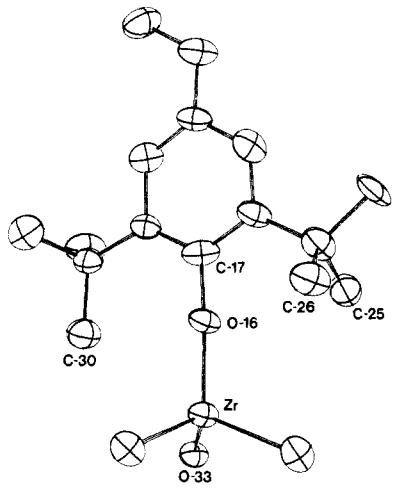

Figure 5. ORTEP view emphasising the coordination geometry of the OAr'–OMe ligand in $Zr(OAr')(OAr'-OMe)(CH_2Ph)_2$.

Table VII. Structural Parameters for Benzyl Ligands in Various Complexes[a]

compd	M-C_α	M-C_1	M-C_2	M-C_6	θ
a	2.27	2.36	2.48		
b	2.13	2.24	2.45		75
Ia	2.28	2.59	2.94	3.35	84
Ib	2.26	2.64	3.16	3.37	88
c	2.58	2.87	3.35	3.57	86

[a] a = $CpMo(CO)_2(4\text{-}CH_3C_6H_4CH_2)$; b = $(C_6Me_5CH_2)Rh[P(O\text{-}i\text{-}C_3H_7)_3]_2$; c = $Cp^*Th(CH_2Ph)_3$. θ refers to the angle M-C_α-C_1 (deg). Distances in angstroms. Carbon atoms are numbered sequentially in the aromatic ring starting with the ipso carbon (C_1). The PhCH_2 carbon is labeled C_α.

hence interesting to speculate if any ground-state Zr···$(CH_3)CMe_2$ interaction is taking place in complex IIc especially in view of the fact that activation of the CH bonds in this group occurs on mild thermolysis.[8d] The ligand can be seen to be perfectly set up geometrically for the ring-closure reaction. However, the distances to this group do not appear to lie in a range that could be considered bonding, and in fact the slightly large Ar-C-CH_3 angle of 118° indicates a repulsive interaction. An explanation of this conformational preference and the possible involvement of the 4-methoxy group (if any) will have to wait for further structural studies.

Structural Characteristics of the Benzyl Ligands. In defining the geometry of the M–CH_2Ph unit a number of parameters are needed to determine the amount of η^n ($n > 1$) bonding to the metal. For a normal σ-bound (η^1) benzyl we can take as our model the parameters found in tetrabenzyltin, $Sn(CH_2Ph)_4$.[5] Here the coordination is almost perfectly tetrahedral about the Sn atom, and the Sn–C–Ph angles are 111° with very little variation (110, 110, 112, and 114°). Altough this precludes any sizeable interaction with the aromatic carbon bound to the methylene group (C_1), it does not itself rule out interactions with the carbons C_2, C_6, or these (ortho) C–H bonds. However, the distances to these positions are too large for any significant interaction. In considering the characteristics of a pure η^3-benzyl we have chosen two examples: $CpMo(CO)_2(\eta^3\text{-}4\text{-}CH_3C_6H_4CH_2)$ and $(\eta^3\text{-}CH_2C_6Me_5)Rh[P(O\text{-}i\text{-}C_3H_7)_3]_2$.[2a,4] In both of these compounds there is structural evidence showing the η^3-bonding mode of the ligands. In these cases the M–C–Ph angles are close to 75° and the M–C distances to the ipso and ortho carbons are short although in both cases longer than M–C_α. This contrasts with the case of $CpMo(CO)_2(\eta^3\text{-}C_3H_5)$ where the allyl group is symmetrically bound with the central M–C distance being slightly shorter than the terminal ones.

Turning now to the compounds obtained in this study we can safely consider the two benzyl ligands in IIc to be of the η^1-type with no interaction between the aromatic ring and the zirconium. In the case of compound I there appears to be one benzyl with a strong η^n ($n > 1$) coordination to the metal, one purely η^1, and an intermediate group, M–C–Ph = 84 (88), 98 (105), and 115° (112) (Ib in parentheses). Concentrating on the first benzyl, Table VII contains a comparison between the bonding parameters of this group in Ia and Ib and those coordinated to Mo and Rh referred to earlier as well as one of the benzyl ligands in $Cp^*Th(CH_2Ph)_3$. These figures imply that the benzyl group in Ia or Ib is in fact interacting with the metal mostly through C_α and then slightly less through C_1 and even less through C_2. Comparison with the data for the Mo and Rh systems show that although the interaction between the aryl group and the zirconium atom is not as pronounced, still there is a significant interaction to C(1) and C(2) so that the bonding is best described as approaching η^3. However, it can be seen that in the case of the thorium compound the interaction is slightly different; compare distances to C_2 vs. C_6. This situation has been described as representing a more symmetrical interaction to the benzyl group (η^4).[6] Although it is possible that this situation could occur for zirconium as well, the parameters for Ib show that in this case the metal is interacting more strongly with one particular side of the aryl ring. Hence, it may be that there is a fundamental difference in the way that actinide and early d-block metals interact with such groups.

An important structural conclusion one can make about the bonding of Zr(IV) metal centers with benzyl groups in compounds such as these is that the multisite bonding is an extremely flexible situation as typified by the large range of Zr–C–Ph angles observed in this study. An entire spectrum of bonding interactions is present between the extreme η^1- and η_3-configurations, and we believe that this flexibility is a contributing factor to some of the problems encountered in the crystallographic studies.

Spectroscopic Characteristics. We have studied both the ^1H and ^{13}C NMR spectral parameters of $Zr(CH_2Ph)_4$

Table VIII. Selected ^1H and ^{13}C NMR Data for Compounds Ia, IIa, $Zr(bz)_4$, Ib, IIb, and $Zr(bz\text{-}F)_4$

	δ (J, Hz)						θ(av), deg
	C_α (^1J)[a]	C_1	$C_{2,6}$	$C_{3,5}$	C_4	$H_{2,6}$	
$Zr(bz)_4$	72.3 (135)	139.3	130.8	128.4	124.4	6.45	92
Ia	74.8 (130)	139.8	129.1	128.6	124.1	6.71	98
IIa	76.8 (125)	142.1	128.9	128.9	123.1	>7.00	
$Zr(bz\text{-}F)_4$	71.1 (133)	134.4 (1.3)[b]	130.0 (7.6)[c]	117.6 (21)[d]	165.1 (240)[e]	6.10	
Ib	73.6 (127)	134.1 (1.2)[b]	129.9 (7.4)[c]	116.1 (21)[d]	160.6 (241)[e]	6.40	100
IIb	75.9 (121)	136.7 (1.2)[b]	129.4 (7.4)[c]	116.2 (22)[d]	159.3 (238)[e]	>6.8	

[a] ^1J(C-H). [b] ^4J(C-F). [c] ^3J(C-F). [d] ^2J(C-F). [e] ^1J(C-F). Carbon atoms are numbered sequentially beginning with the ipso carbon as C_1.

and $Zr(CH_2PhF)_4$ as well as of I and II to see if it is possible to differentiate the two types of bonding. Although in both the solid-state structure of $Zr(CH_2Ph)_4$ and I there are considerable differences between various benzyl ligands, we have been unable to "freeze out" these differing groups either in the ^1H or ^{13}C NMR spectra of these compounds. Hence it appears that in solution either facile exchange of differing benzyl groups takes place or else all groups are equivalent. Due to this unfortunate situation one is left only with a comparison of spectroscopic data with the *average* bonding parameters of the benzyl groups as determined by X-ray crystallography. Comparing the data in Table VIII, it appears that the most significant changes are in the chemical shift of the ortho protons of the benzyl group and to a lesser extent the chemical shift and coupling constant of the α-carbon. In the cases where significant amounts of π-bonding between the aryl group and zirconium is taking place, the ortho protons of the benzyl groups tend to shift upfield of the normal aromatic region to significantly higher chemical shifts. This effect was also observed in $Cp^*Th(CH_2Ph)_3$.[6] In the case of compound II this signal moves back into the "normal" aromatic region of δ 6.8–7.5. The only other significant changes are a slight change in the chemical shift of the α compound and in the coupling constant $^1J(C_\alpha\text{–}H)$. The chemical shift changes of this carbon atom cannot be used as any indication of a bonding change as it may be caused by the sequential introduction of the aryl oxide groups onto the metal. However, the increase in the coupling constant parallels a decrease in the Zr–C–Ph angle and can be interpreted as reflecting the increasing amount of sp^2 character of the α-carbon as this angle decreases.

Hence, it appears that at least for these early-transition-metal systems, the only reliable spectroscopic indication of significant π-interaction to benzyl ligands is the chemical shift of the ortho protons and also the coupling constant of the α-CH_2 group. We note that based on reported spectroscopic data the compounds $Cp^*Zr(CH_2Ph)_3$ and Zr (tritox)$(CH_2Ph)_3$[9,12] should have π-bonding between the benzyl groups and zirconium. However, at the present time no structural data has been reported on these compounds.

It is unfortunate that the solid-state structure of Ia is poor. An interesting comparison is to see what effect the introduction of a fluoro substituent has on the π-bonding of the aryl group of the benzyl ligand. However, it can be seen that the effect appears negligible, the average Zr–C–Ph angles angles only differing by 2° for Ia and Ib. Furthermore the spectroscopic data also implies that the fluoro group has little effect on the strength of the π-interaction.

Experimental Section

Synthesis of $Zr(OAr')(CH_2Ph)_3$ (Ia). To a toluene solution of $Zr(CH_2Ph)_4$ was added 2,6-di-*tert*-butylphenol (1 equiv), and the mixture was allowed to stand for 6 h. Removal of solvent, addition of hexane, and cooling to −15 °C gave yellow-brown crystals of the product in good yield. Extended exposure to light causes darkening of the compound. ^1H NMR spectrum (30 °C, C_6D_6): δ 1.37 (s, C_6H_3-*t*-Bu), 2.32 (s, CH_2Ph), 6.71 (m, ortho), 7.0–7.4 (m, other aromatic signals). $Zr(OAr')(C_2Ph\text{-}Fe)_3$ (Ib) was synthesized by identical methods using $Zr(CH_2PhF)_4$. ^1H NMR spectrum (30 °C, C_6D_6) δ 1.37 (s, C_6H_3-*t*-Bu), 2.08 (s, CH_2Ph), 6.4 (m, ortho), 7–7.4 (m, other aromatic signals).

Synthesis of $Zr(OAr')_2(CH_2Ph)_2$ (IIa). The addition of greater than 2 equiv of 2,6-di-*tert*-butylphenol (HOAr') to $Zr(CH_2Ph)_4$ in toluene results after 24 h in the formation of the product. Careful addition of hexane and cooling allows the isolation of pale yellow crystals of II which can be washed with hexane and dried under vacuum. Anal. Calcd for $ZrC_{42}H_{56}O_2$: C, 73.77; H, 8.25. Found: C, 73.60; H, 8.13. ^1H NMR (30 °C, C_6D_6): δ 1.45 (s, C_6H_3-*t*-Bu), 2.84 (s, CH_2Ph), 7–7.5 (m, CH_2Ph and C_6H_3-*t*-Bu). $Zr(OAr')_2(CH_2PhF)_2$ (IIb) was synthesized similarly from $Zr(CH_2PhF)_4$. ^1H NMR (30 °C, C_6D_6): δ 1.40 (s, C_6H_3-*t*-Bu), 2.70 (s, CH_2Ph), 6.8–7.1 (m, CH_2Ph and C_6H_3-*t*-Bu). $Zr(OAr')(OAr'\text{-}OMe)(CH_2Ph)_2$ (IIc) was synthesized by addition of 1 equiv of 2,6-di-*tert*-butyl-4-methoxyphenol (HOAr') to a benzene solution of Ia at 25 °C and allowing the mixture to stand 24 h. Removal of solvent and addition of hexane gave the product as pale yellow crystals. ^1H NMR (30 °C, toluene-d_8): δ 1.45 (s, OC_6H_3-*t*-Bu_2 and $OC_6H_2OMe(t\text{-}Bu)_2$, 2.83 (s, CH_2Ph), 3.50 (s, OMe), 6.9–7.2 (m, aromatics).

X-ray Structural Determination for $Zr(OAr')(CH_2Ph)_3$ (Ia). A crystal of Ia of maximum dimension 0.26 mm was affixed to a glass fiber using silicone grease and transferred to a Picker goniostat where it was cooled to −160 °C for characterization and data collection. The crystal was maintained in an inert-nitrogen atmosphere at all times. The experimental techniques, low-temperature device, and diffractometer system used have been described in detail previously.[13] A systematic search for a limited hemisphere of reciprocal space revealed a set of diffraction maxima of monoclinic symmetry with extinctions $h + k = 2n + 1$ for hkl and $l = 2n + 1$ for $h0l$, consistent with space groups $C2/c$ or Cc. Complete crystal data are presented in Table I. Although the crystal apeared well-formed, less than half of the data were considered observed, using the criteria $I^{obsd} > 2.33\sigma(I^{obsd})$. The low percentage is atypical of low-temperature data and usually indicative of disorder or twinning.

The structure was readily solved in the centrosymmetric space group $C2/c$ by a combination of direct methods and Fourier techniques. A difference Fourier phased on the non-hydrogen parameters yielded chemically reasonable positions for all hydrogen atoms excluding those on C(17) and C(21). Attempts to refine the hydrogen positions were unsuccessful, as several tended to "drift" substantially from the expected location. For this reason all hydrogens (excluding those not located) were included as fixed atom contributors in the final cycles of the full-matrix least-squares refinement. Attempts to refine in the noncentric space group Cc did not lead to improvement in the residuals, indicating the centrosymmetric space group is the proper choice. A final difference Fourier was featureless, the largest peak being 0.72 e/Å^3 located adjacent to the Zr atom. Examination of the thermal parameters for the final model reveals several which are quite aniosotropic. Psi scans for several reflections indicated that there was no significant absorption problem, a typical cause of poorly behaving thermal parameters. It can only be assumed that the large esd's and thermal parameters are due to a slight, but uncharacterizable, disorder in the benzyl groups. It is interesting to note that problems were encountered with the refinement of the structure of $Zr(CH_2Ph)_4$,[5] although a full report of this structure determination has not yet appeared in the literature.

X-ray Structural Determination for $Zr(OAr')(CH_2PhF)_3$ (Ib). Because of persistent problems with the structure of Ia, a sample of Ib was mounted and characterized as above. The structure was solved by direct methods (MULTAN78) and Fourier techniques, and all hydrogens were located and refined isotropically. No absorption correction was performed. A final difference Fourier was featureless, the largest peak being 0.23 e/Å^3.

X-ray Structural Determination for $Zr(OAr')(OAr'\text{-}OMe)(CH_2Ph)_2$ (IIc). Examination of a sample of IIc showed that most of the crystals appeared to have imperfections and while transparent were not of good quality. One of the larger crystals was cleaved to obtain a transparent fragment with no apparent imperfections, and careful examination of the sample on the goniostat indicated good crystal quality. All handling was done in an inert atmosphere, and the sample was cooled to −160 °C before characterization and data collection.

A systematic search of a limited hemisphere of reciprocal space yielded a set of diffraction maxima with monoclinic symmetry and extinctions corresponding to the unique space group $P2_1/n$. The Zr atom, both O atoms, and 24 carbon atoms were clearly

(12) Wolczanski, P. T.; Bercaw, J. E. *Organometallics* **1982**, *1*, 793.

(13) Huffman, J. C.; Lewis, L. N.; Caulton, K. G. *Inorg. Chem.* **1980**, *19*, 2755.

visible in an E map (MULTAN78), and all remaining atoms were located in subsequent difference Fourier synthesis. Hydrogen atoms were subsequently located and refined. While the positions of the hydrogen atoms are not well determined, they are qualitatively correct and converged properly. Refinement was blocked due to the large number of parameters.

A final difference Fourier was featureless, the largest peak being 0.45 e/Å^3.

Acknowledgment. We thank the National Science Foundation (Grant CHE-8219206) for support of this work.

Registry No. Ia, 95531-69-4; Ib, 95552-55-9; IIa, 94598-00-2; IIb, 95531-70-7; IIc, 95531-71-8; $Zr(CH_2Ph)_4$, 24356-01-2; $Zr(CH_2PhF)_4$, 34072-35-0; 2,6-di-*tert*-butylphenol, 128-39-2; 2,6-di-*tert*-butyl-4-methoxyphenol, 489-01-0.

Supplementary Material Available: Listings of isotropic thermal parameters and fractional coordinates for Ia and Ic, fractional coordinates for hydrogen atoms for Ia and Ib, and anisotropic thermal parameters, bond distances and angles, and observed and calculated structure factors for Ia-c (62 pages). Ordering information is given on any current masthead page.

The PdO-Catalyzed Reaction between $[Re_2(CO)_{10}]$ and Isocyanides

Gillian W. Harris and Neil J. Coville*

Department of Chemistry, University of the Witwatersrand, Johannesburg 2001, Republic of South Africa

Received September 10, 1984

The reaction between $[Re_2(CO)_{10}]$ and RNC (R = Me, *t*-Bu, $C_6H_5CH_2$, C_6H_{11}, 2,6-$Me_2C_6H_3$) is catalyzed by PdO to yield the products $[Re_2(CO)_{10-n}(CNR)_n]$ (n = 1-3, R = *t*-Bu, $C_6H_5CH_2$, C_6H_{11}; n = 1-4, R = Me, 2,6-$Me_2C_6H_3$) rapidly and in moderate to excellent yields. The reaction occurs via stepwise replacement of CO groups and mixed-isocyanide derivatives can thus be synthesized, e.g., $[Re_2(CO)_8(CNBu\text{-}t)(CNC_6H_3Me_2\text{-}2,6)]$. The products have been completely characterized by IR and NMR spectroscopy and for certain derivatives by mass spectrometry. A correlation between the above spectroscopic parameters and the product geometry, after crystallographic determination of the structures of pertinent substituted derivatives, has been made. In all products the isocyanide ligands occupy cis equatorial positions on either the same or different Re atoms, indicating the dominance of electronic rather than steric factors in the control of the final product geometry. Labeling studies using $[Re(^{13}CO)_{12}]$ indicate that the PdO-catalyzed reaction to yield $[Re_2(CO)_9(CNBu\text{-}t)]$ occurs via a CO dissociative mechanism rather than a process involving metal-metal bond cleavage.

Introduction

Transition-metal cluster complexes in both high and low oxidation states have been actively studied since the early 1960s.[1] Part of the justification for this activity has arisen from the suggestion that metal clusters can be viewed as bridges between molecular and solid-state chemistry[2] and further that cluster catalysis might give information on multi-atom (surface) catalysis.[3] As a prerequisite to establishing whether the above hypotheses are justified a fundamental understanding of the chemistry of cluster reactions is required and is being developed.[4]

Some years ago we commenced a study of the substitution reactions of $[M_2(CO)_{10}]$ (M_2 = Mn_2, Re_2, MnRe) using catalysts to induce CO displacement by phosphines and isocyanide ligands.[5] This system was chosen as a model for an investigation of the chemical reactivity of larger clusters (trimers, tetramers, etc.) as it contains one M-M bond and no bridging ligands (in the ground state).[6] Further, the use of catalysts could allow for the synthesis of $[M_2(CO)_{10-n}L_n]$ ($n > 1$) complexes under conditions in which M-M bond cleavage is eliminated or greatly reduced. Indeed, when this study was commenced, the mechanism of the thermal substitution reaction $[Mn_2(CO)_{10}] + PPh_3 \rightarrow [Mn_2(CO)_9(PPh_3)] + CO$ was postulated to occur via Mn-Mn bond cleavage rather than a CO dissociative process[8] and it was anticipated that a lower temperature catalytic pathway would eliminate the possibility of the Mn-Mn cleavage route. (Recent labeling and other studies[9] have, however, now indicated that the thermal, high-temperature reaction occurs via a dissociative mechanism.)

This publication describes the catalyzed synthesis of a series of $[Re_2(CO)_{10-n}(CNR)_n]$ (n = 1-4; R = alkyl and aryl isocyanide) complexes from $[Re_2(CO)_{10}]$ and RNC. Although the analogous Mn derivatives have been studied,[10] only one previous report of an analogous Re-RNC complex—a brief mention of the Raman spectrum of $[Re_2(CO)_9(CNMe)]$—has been made.[11] These Re and Mn complexes are of particular interest as it is hoped that the stereochemistry of the substituted products will eventually

(1) See, for example: Johnson, B. F. G., Ed. "Transition Metal Clusters"; Wiley: New York, 1980.
(2) Muetterties, E. L.; Rhodin, T. N.; Band, E.; Brucker, C. F.; Pretzer, W. R. *Chem. Rev.* **1979**, *79*, 91.
(3) Muetterties, E. L.; Krause, M. J. *Angew. Chem., Int. Ed. Engl.* **1983**, 22, and references cited therein.
(4) Muetterties, E. L. *J. Organomet. Chem.* **1980**, *200*, 177.
(5) Albers, M. O.; Coville, N. J.; Singleton, E. *J. Chem. Soc., Chem. Commun.* **1982**, 96.
(6) Churchill, M. R.; Amoh, K. N.; Wasserman, H. J. *Inorg. Chem.* **1981**, *20*, 1609.
(7) Haines, L. I. B.; Hopgood, P.; Poë, A. J. *J. Chem. Soc. A* **1968**, 421.
(8) Wawersik, H.; Basolo, F. *Inorg. Chim. Acta* **1969**, *113*, 3.
(9) (a) Sonnenberger, D.; Atwood, J. D. *J. Am. Chem. Soc.* **1980**, *102*, 3484. (b) Schmidt, S. P.; Trogler, W. C.; Basolo, F. *Inorg. Chem.* **1982**, *21*, 1698. (c) Coville, N. J.; Stolzenberg, A. M.; Muetterties, E. L. *J. Am. Chem. Soc.* **1983**, *105*, 2500.
(10) Albers, M. O.; Coville, N. J. *S. Afr. J. Chem.* **1982**, *35*, 139 and references cited therein.
(11) Prasad, P. N. *Spectrochim. Acta, Part A* **1977**, *33A*, 335.

0276-7333/85/2304-0908$01.50/0